

81-3-169

# DEUTSCHES ELEKTRONEN-SYNCHROTRON **DESY**

DESY 81-008  
January 1981

CHARGED HADRON PRODUCTION IN  $e^+e^-$  ANNIHILATION

IN THE  $\tau$  AND  $\tau'$  REGION

by

*LENA Collaboration*

NOTKESTRASSE 85 · 2 HAMBURG 52

DESY behält sich alle Rechte für den Fall der Schutzrechtserteilung und für die wirtschaftliche Verwertung der in diesem Bericht enthaltenen Informationen vor.

DESY reserves all rights for commercial use of information included in this report, especially in case of apply for or grant of patents.

To be sure that your preprints are promptly included in the  
HIGH ENERGY PHYSICS INDEX ,  
send them to the following address ( if possible by air mail ) :

DESY  
Bibliothek  
Notkestrasse 85  
2 Hamburg 52  
Germany

CHARGED HADRON PRODUCTION IN  $e^+e^-$  ANNIHILATION IN THE T AND T'

REGION †)

LENA Collaboration

B. Niczyporuk, T. Zełudziejewicz

Institute of Nuclear Physics, Cracow, Poland

K.W. Chen, R. Hartung

Department of Physics, Michigan State University, East Lansing,  
MI, USA<sup>§</sup>

G. Folger, B. Lurz, H. Vogel<sup>†</sup>, U. Volland, H. Wegener

Physikalisches Institut der Universität Erlangen-Nürnberg, Germany

J.K. Bienlein, R. Graumann, J. Krüger, M. Leißner, M. Schmitz

Deutsches Elektronen-Synchrotron DESY, Hamburg, Germany

F.H. Heimlich, R. Nernst, A. Schwarz, U. Strohbusch, H.-J. Trost,  
P. Zschorsch

I. Institut für Experimentalphysik der Universität Hamburg, Germany

A. Engler, R.W. Kraemer, F. Messing, C. Rippich, B. Stacey,

S. Yousef

Department of Physics, Carnegie-Mellon University, Pittsburgh, PA,  
USA<sup>§§</sup>

A. Fridman

DPPhE, CEN de Saclay, France

G. Alexander, A. Av-Shalom, G. Bella, Y. Gnat, J. Grunhaus

Department of Physics and Astronomy, Tel-Aviv University, Israel\*

E. Hörber<sup>††</sup>, W. Langguth<sup>†††</sup>, M. Scheer

Physikalisches Institut der Universität Würzburg, Germany

†) submitted to Z. Phys. C

+ now at MPI Munich, Germany

++ now at MBB Munich, Germany

+++ now at DESY, Hamburg, Germany

\$ partially supported by the US National Science Foundation

\$\$ partially supported by the US Department of Energy

\* partially supported by the Israel Academy of Sciences and  
Humanities

Abstract

Charged hadron production in  $e^+e^-$  annihilation is studied in the 7 to 10 GeV CM energy region and at the T (9.46) and T' (10.01) resonances with the LENA detector at DORIS. The statistical moments of the charged multiplicities are studied. The data show KNO scaling behaviour and suggest the presence of long range correlations. An average charged multiplicity rise of  $\Delta n(T) = 0.55 \pm 0.19$  and  $\Delta n(T') = 1.26 \pm 0.29$  over the continuum is observed for the T and T' direct decays. The jet structure of the T and T' direct decays is investigated using the charged particles. The polar angular distributions of the jet axis behave like  $1 + \alpha(T) \cos^2 \Theta$  with  $\langle \alpha(T) \rangle_T = 0.7 \pm 0.3$  and  $\langle \alpha(T) \rangle_{T'} = 0.6 \pm 0.4$ . The  $\langle \alpha(T) \rangle_T$  value is in agreement with the QCD vector gluon assignment and excludes scalar gluons by more than four standard deviations.

## I. Introduction

The study of hadron production in  $e^+e^-$  annihilation in the  $\Upsilon$  (9.46) region has proven to be a useful tool in the understanding of the decay mechanism of bound quark-antiquark ( $q\bar{q}$ ) states. In particular the comparison between the  $\Upsilon$  resonance decay data and those of the nearby continuum has shown that many features are consistent with the lowest order QCD 3 gluon process [1-4]. So far very little information has been reported on the  $\Upsilon'$  (10.01) decay into hadrons [3,5]. The  $\Upsilon'$  is expected to decay into hadrons via the 3 gluon process and also through intermediate states containing bound  $b\bar{b}$  systems. Some of these systems decay into 3 gluons, among them the  $\Upsilon$  resonance, and some into 2 gluons. Thus,  $\Upsilon$  and  $\Upsilon'$  data taken in the same experiment afford the possibility to compare their decay properties.

Here we present results on the multiplicity and jet structure of the charged hadrons from a large statistics  $e^+e^-$  annihilation experiment performed in the  $\Upsilon$  and  $\Upsilon'$  energy region. In Section II we describe the experimental data selection and the analysis methods. The charged multiplicities are studied in Section III and compared to those reported for  $pp$  and  $p\bar{p}$  collisions. The geometrical jet structure of the  $\Upsilon$  and  $\Upsilon'$  hadronic decays is investigated in Section IV. These data are also compared with continuum data.

## II. Experimental Procedure

The data were taken in the CM energy range of 7-10 GeV including the  $\Upsilon$  and  $\Upsilon'$  resonances using the non-magnetic LENA detector at DORIS. This detector is described in details elsewhere [4,6,7]. The charged particles were detected by three cylindrical double drift chambers giving the track direction and covering 86% of  $4\pi$  solid angle. Two scintillation hodoscopes were used in the trigger as well as energy information obtained from NaI and lead-glass blocks (178 in total).

All the candidates for hadronic events were scanned by physicists to remove background events such as beam gas interactions, Bhabha scattering and cosmic rays. In the present analysis we have restricted ourselves to events having at least three charged particles identified as hadrons. For the multiplicity study we use

the data taken in the continuum at 7.4-10 GeV, while for the jet analysis we confine ourselves to the data on the  $\Upsilon$  and  $\Upsilon'$  resonances and at their nearby energies. The continuum data were divided into five CM energy intervals as specified in Table 1. This table also gives the average CM energy for each interval, the number of events, and the corresponding accumulated luminosities.

In order to study the properties of the  $\Upsilon$  and  $\Upsilon'$  hadronic decay we must first subtract the contribution of the continuum  $\sigma_{\text{off}}^h$ . Furthermore we also subtract the vacuum polarisation (decay via a virtual photon) contribution  $\sigma_{\text{vp}}^h$  which has the same behaviour as the continuum. In the  $\Upsilon$  case this leaves us with the so called direct hadronic decay channel mediated by the 3-gluon QCD mechanism. This subtraction method when applied to the  $\Upsilon'$  data, does not isolate the 3 gluon contribution since the  $\Upsilon'$  has additional decay channels. These additional channels will end in final states containing also  $b\bar{b}$  bound systems some of which (in particular the  $\Upsilon'$ ) decay into 3 gluons and some into 2 gluons. Here we will study the  $\Upsilon'$  decay using the same subtraction procedure applied to the  $\Upsilon$ . In as much as the 2-gluon  $\Upsilon'$  decay channels are important, deviations between the  $\Upsilon'$  and  $\Upsilon$  decay may be detected. In what follows we will refer both to the  $\Upsilon$  and  $\Upsilon'$  subtracted samples as the direct decay data keeping in mind, however, that 2 gluon decay contributions may also be present in the  $\Upsilon'$  sample.

The direct decay cross sections are calculated using the expression

$$\begin{aligned}\sigma_{\text{dir}}^h &= \sigma_{\text{on}}^h - \sigma_{\text{off}}^h - \sigma_{\text{vp}}^h \\ &= \sigma_{\text{on}}^h - \sigma_{\text{off}}^h - (\sigma_{\text{on}}^h - \sigma_{\text{off}}^h) \cdot R \cdot B_{\mu\mu}^h \cdot (1 - 3B_{\mu\mu}^h)^{-1}\end{aligned}$$

where  $R = \sigma_{\text{off}}^h / \sigma_{\mu\mu}^h$  was taken to be  $(3.7 \pm 0.4)$ .

The subscripts indicate the observed cross section on and off the resonance for hadron production (h). To calculate  $\sigma_{\text{dir}}^h$  we use our measured value of the mu-pair branching ratio  $B_{\mu\mu}^h(\Upsilon) = (3.5 \pm 1.4)\%$  [4]. In the case of the  $\Upsilon'$ , only an upper limit of 3.8% has been determined for  $B_{\mu\mu}^h(\Upsilon')$ . We used  $B_{\mu\mu}^h(\Upsilon') = 1.7\%$  which is consistent with theoretical predictions [8] and with the deduced value of ref.9.

Since the main subtraction is due to the continuum contribution, the direct samples are almost insensitive to the value of  $B_{\mu\mu}$  used.

### III. Charged Multiplicity

Since the acceptance for charged particles in our detector is less than 100% (the geometrical acceptance is 86% of  $4\pi$ ) we observe events with both even and odd numbers of charged prongs whereas clearly only an even number can be produced. The true charged multiplicity distribution can be deduced from the data knowing the acceptance properties of the detector. Denoting by  $F_n$  the true number of events with  $n$  (even) outgoing charged particles, the observed distribution  $f_m$  is given by [10]

$$f_m = \sum_n P_{mn} F_n.$$

Here  $m = 0, 1, 2, \dots$  is the observed number of charged tracks. The matrix element  $P_{mn}$  represents the probability that a produced  $n$  prong event will be observed with  $m$  charged particles. Note that  $m$  can be larger than  $n$  due to photon conversion in the beam pipe. Since  $m$  can have even and odd values, one has more equations than unknowns. We therefore solve the equations using the least square method where the  $P_{mn}$  are determined from Monte Carlo calculations.

To determine  $P_{mn}$  for the continuum data, Monte Carlo events were generated according to the 2 jet  $q\bar{q}$  model of Field and Feynman [11] with the inclusion of the charmed quark. For the  $\tau$  and  $\tau'$  direct decay we used a 3 gluon QCD decay matrix element [12] and assumed that gluons fragment like quarks. In this way two sets of  $P_{mn}$  probabilities were calculated, one for the continuum and one for the direct decays. In this calculation we took into account our various detection efficiencies, the deficiencies of the pattern recognition program and photon conversions in the beam pipe. It should be noted that the  $P_{mn}$  probabilities do not depend on the charged multiplicity distribution assumed in Monte Carlo programs. The  $P_{mn}$  do depend somewhat however on the assumed Monte Carlo ratio of neutral to charged particles at each multiplicity. This ratio determines the number of photons produced which then have a 5% probability to convert in the beam pipe. Since this neutral to charged ratio is

experimentally not well known, we have taken the values as obtained from the Field and Feynman fragmentation functions.

Fitting our observed multiplicity distributions for  $m \geq 3$ , we obtain the true (unfolded) distribution. The contribution of 0 and 2 prongs to the unfolded distributions were estimated by assuming that their relative fractions are the same as in the generated Monte Carlo events. Table 2 shows some statistical moments derived from the unfolded distributions, namely, the average charged multiplicity  $\langle n \rangle$ , its dispersion  $D = \sqrt{\langle n^2 \rangle - \langle n \rangle^2}$  and its Mueller moment [13]  $f_2^- = \langle n_-(n_- - 1) \rangle - \langle n_- \rangle^2$  where  $n_- = n/2$ . The errors given in this table are statistical only. For comparison we also present the averages of the observed distributions which are significantly different from the unfolded ones. We note that the dependence of  $\langle n \rangle$  in the continuum increases faster than  $\langle n \rangle = 2.1 + 0.85 \ln s$  (see Fig. 1) which describes the  $e^+e^-$  data below 7 GeV [14]. A better agreement is obtained with the QCD prediction [15]

$$\langle n \rangle = a + b \exp[c(\ln(s/\Lambda^2))^{1/2}], \quad \Lambda = 0.5 \text{ GeV}$$

using the parameters  $a = 2.38 \pm 0.09$ ,  $b = 0.04 \pm 0.01$  and  $c = 1.92 \pm 0.07$ , obtained from a fit including high energy ( $\sqrt{s} > 9 \text{ GeV}$ ) data [16]. In the 9 GeV region, our data points, as well as those obtained from other experiments, lie somewhat higher than the QCD prediction (Fig. 1).

For the  $\tau$  and  $\tau'$  we obtain higher average multiplicity and dispersion values than at their nearby continuum. The multiplicity of the  $\tau$  direct decay of  $\langle n \rangle = 8.12 \pm 0.11$  is consistent with previously reported values [1-3]. This average is within the range of values predicted by QCD calculations [17,18]. It is worthwhile to note that the unfolded multiplicity of the  $\tau'$  is higher by  $0.81 \pm 0.28$  than that of the  $\tau$ . This difference can be accounted for by the  $\tau'$  chain decays such as  $\tau' \rightarrow \pi^+ \pi^- \tau$  discussed elsewhere [9].

As in hadron-hadron interactions we observe a linear dependence [19] between  $D$  and  $\langle n \rangle$ . This is illustrated in Fig. 2a which presents our results together with those obtained with the PLUTO detector [16]. A fit to this distribution with  $D = A\langle n \rangle + B$  yields

\* The decays  $K_S^0 \rightarrow \pi^+ \pi^-$  are not excluded.

the values  $A = 0.33 \pm 0.03$  and  $B = 0.23 \pm 0.23$ . For large  $s$ ,  $D/\langle n \rangle$  approaches the value  $A$  which is nearly equal to the  $D/\langle n \rangle$  ratios found in  $\bar{p}p$  annihilation [21]. In Table 2 we also present our  $D/\langle n \rangle$  values at different CM energies; these can be compared with the dual unitarization model [22,23]. This model relates  $D/\langle n \rangle$  for  $e^+e^-$  annihilation with  $pp$  interactions through [23]

$$\left[ \frac{D(s)}{\langle n(s) \rangle} \right]_{e^+e^-} = \sqrt{s} \left[ \frac{D(\bar{s})}{\langle n(\bar{s}) \rangle} \right]_{pp}$$

where  $\sqrt{s} = 0.2 \sqrt{\bar{s}}$ . In our energy range this model predicts a value of  $D/\langle n \rangle = 0.75$  which obviously is higher by a factor  $\sim 2$  than our experimental values.

The  $D/\langle n \rangle$  ratio has recently also been studied in terms of the QCD model considering single quark and gluon jets [15]. To compare our data at the continuum with this approach, we assume that the two produced quarks fragment independently. In this way the QCD predicted ratio [15] is  $D/\langle n \rangle = 0.61$  which is still higher than our continuum data.

In Fig. 2b we present the  $f_2^-$  moments as a function of  $\langle n \rangle$ . These  $f_2^-$  have a negative sign similar to  $\bar{p}p$  annihilation whereas in other hadron reactions they have a positive value for  $\langle n \rangle \geq 4$  [20]. The  $s$  dependence of  $f_2^-$  is sensitive to the presence of long range correlations [24], a feature which is also expected by QCD [15]. The  $s$  range of our data is however too narrow to study the detailed energy dependence of  $f_2^-$ . We thus plot our data in the so called KNO form [25], namely  $\langle n \rangle P_n$  versus  $n/\langle n \rangle$  (Fig. 3). Here  $P_n$  is the probability to observe an  $n$  prong event. The KNO scaling hypothesis states that all data points for a given type of reaction should be distributed on a universal curve independent of the CM energy.

Fig. 3 shows indeed that our data at various  $s$  values lie essentially on the same curve, nearly identical to the  $\bar{p}p$  annihilation data. This fact has been noted previously [16]. An equivalent form of the KNO scaling hypothesis is the requirement that the reduced moments  $c_q = \langle n^q \rangle / \langle n \rangle^q$  are independent of  $s$  [24]. This leads to  $f$  proportional to  $\langle n \rangle^2$ . The fact that  $\langle n \rangle$  varies as fast as  $\ln s$  [16] means that  $f_2^-$  varies at least as  $(\ln s)^2$  which implies the presence of a long range correlation between the produced particles [15,24].

#### IV. Hadron Jet Analysis

In contrast to the continuum, the  $\Gamma$  direct decay is expected to be mediated by three gluons. The outgoing hadrons should then emerge in three jets. However due to the relatively low CM energy, these three jets are in general not resolvable. Nevertheless the space configuration of the direct decay events should be different from the 2 jet structure which describes the continuum at similar energies. This difference has been studied in earlier limited statistics experiments [1-3]. The jet structure of the  $\Gamma'$  is somewhat more complex due to the presence of several additional decay modes as mentioned above. The  $\Gamma'$  decay into 3 gluons and the decay chain  $\Gamma' \rightarrow \gamma\gamma\Gamma, \Gamma \rightarrow 3g$  will have the same behaviour as that of the  $\Gamma$  since their mass values are close. Furthermore one of the  $P$  states ( $1^3P_1$ ) of the  $\Gamma'$  radiative decay has a 3-jet like decay mode. The 2 gluon decay channels should be similar to the 2 jet structure of the continuum.

The gross features of the angular structure of the continuum and the resonance direct decays is shown in Fig. 4. In this figure we present the distributions of  $\cos \delta$  where  $\delta$  is the opening angle between pairs of charged tracks. The continuum data are enhanced near  $\cos \delta = \pm 1$ . These distributions are well described by the 2-jet  $q\bar{q}$  Monte Carlo calculations. The  $\Gamma$  and  $\Gamma'$  direct decay distributions in  $\cos \delta$  are appreciably less enhanced than the continuum. The distributions for the  $\Gamma$  and  $\Gamma'$  are essentially identical and are well described by the 3 gluon Monte Carlo prediction.

For a quantitative measure of the jet structure we use a thrust-like quantity since the momenta of the charged particles are not measured in our experiment. To this end we define

$$T' = \max_{i=1}^N \frac{\sum_{j=1}^N |\cos \theta_{ij}|}{N}$$

where  $\theta_{ij}$  are the polar angles of the charged tracks with respect to the axis which maximizes  $\sum_{i=1}^N |\cos \theta_{ij}|$ . Here  $N$  is the number of charged tracks in a given event. The quantity  $T'$  thus defined is

strongly correlated to the normal thrust variable  $T_{ch}$  which utilizes the momenta of the charged particles. This correlation is shown in Fig. 5 which presents a scatter plot of  $T'$  versus  $T_{ch}$  for 3 gluon Monte Carlo events generated at 9.4 GeV. As seen, the points are clustered along a line parallel and near to the diagonal. We note however, that  $T'$  tends to be smaller than  $T_{ch}$ . A similar correlation is found for the  $q\bar{q}$  Monte Carlo events (not shown).

The normalized experimental  $T'$  distributions of the  $\tau$  and  $\tau'$  direct decays and the nearby continuum are shown in Fig. 6. These distributions are compared with the  $q\bar{q}$  and 3 gluon Monte Carlo events. The continuum data are adequately described by the two jet Monte Carlo prediction whereas the direct decay data are better described by the 3 gluon mechanism. Within the present statistics the  $T'$  decay spatial configuration appears not to be affected by its additional non 3 gluon decay modes. The average values of  $T'$  are given in Table 3. One notices that  $T'$  for the  $\tau'$  and  $\tau$  direct decay are nearly equal and significantly lower than those of the continuum.

Hadron final states in one photon  $e^+e^-$  annihilation are mediated by  $q\bar{q}$  production with a subsequent fragmentation into hadrons. For spin 1/2 pointlike quarks, the distribution in the polar angle  $\theta$  of the quark with respect to the  $e^+e^-$  direction is given by

$$d\sigma/d(\cos\theta) \sim 1 + \cos^2\theta.$$

The two jets due to these quarks should follow closely the original quark direction which we measure by the thrust axis. In Fig. 7a we present the angular distribution of the thrust axis for the combined continuum data from 9.2 to 10 GeV. This distribution is corrected for our detection efficiencies. The data were fitted with the expression  $1 + \alpha \cos^2\theta$  giving  $\alpha = 0.7 \pm 0.1$  (full line in Fig. 7a), a value lower than that expected for free quarks. For comparison we also show in this figure the  $(1 + \cos^2\theta)$  behaviour (dashed line).

For the  $\tau$  direct decay into 3 vector gluons QCD predicts [26] a thrust angular distribution of

$$d\sigma/d(\cos\theta) \sim 1 + \alpha(T)\cos^2\theta.$$

This  $\alpha(T)$  folded with the QCD predicted differential  $T$  distribution gives an average value of [26],  $\langle\alpha(T)\rangle = 0.39$ . In the case of a 3 scalar gluon decay the average is expected to be  $\langle\alpha(T)\rangle = -0.995$  [27]. Our experimental  $dN/d \cos\theta$  distributions for the  $\tau$  and  $\tau'$  direct decay are shown in Fig. 7b and 7c. The distributions were corrected for acceptance. The correction factors were found to be essentially independent of the angular distribution assumed for the Monte Carlo program. We note that the angular distribution obtained for the  $\tau'$  data is similar to that of the  $\tau$ . Fitting these distributions we obtain for the  $\tau$  and  $\tau'$  the values  $\langle\alpha(T)\rangle_{\tau} = 0.7 \pm 0.3$  and  $\langle\alpha(T)\rangle_{\tau'} = 0.6 \pm 0.4$ . The results of these fits are represented in Fig. 7b and 7c by continuous lines. In the same figures we also present the predicted distributions for vector (dashed lines) and scalar (dashed dotted lines) gluons. The fitted  $\langle\alpha(T)\rangle_{\tau}$  is in agreement within 1 standard deviation with the QCD vector assignment to the gluon. A scalar assignment to the gluon is excluded by more than 4 standard deviations.

## V. Conclusions

In this work we have studied the multiplicity and the jet structure of charged hadrons produced in  $e^+e^-$  annihilation in the energy range of 7 to 10 GeV. At these energies the average multiplicity of the continuum rises with energy ( $\sqrt{s}$ ) faster than  $\ln s$ . Similar to hadron-hadron reactions we observe a linear relation between the dispersion  $D$  and the average charged multiplicity  $\langle n \rangle$ . This allows us to estimate  $D/\langle n \rangle = 0.33 \pm 0.03$  for large  $s$  which is inconsistent with the Dual Unitarization Model as well as with some QCD estimates. Our multiplicity data presented in the KNO form are distributed on a curve similar to that obtained from  $pp$  annihilations. This scaling behaviour in conjunction with the fast increase of  $\langle n \rangle$  with the CM energy supports the existence of a long range correlation between the produced hadrons.

The average charged multiplicity of the  $\tau$  and  $\tau'$  direct decays is

found to be higher than the nearby continuum value, as expected from a QCD decay mechanism of bound quark states. Whereas this increase is only about half a unit for the  $T$ , it is  $1.26 \pm 0.29$  for the  $T'$ . This higher value for the  $T'$  can readily be understood by the additional  $T' \rightarrow \pi^+ \pi^- T$  decay mode. At the same time the values for  $D$  and the moment  $f_2^-$  of the direct decays plotted against  $\langle n \rangle$  present the same behaviour as the continuum.

The jet structure of our charged hadron data has been studied with a thrust-like quantity which utilizes only the direction of the particles. This quantity is found to be strongly correlated to the conventional thrust which requires also the particle momenta. The  $T$  direct decay spatial configuration is appreciably different from that of the continuum, and is consistent with QCD expectations. In the case of the  $T'$ , the data are better described by the three gluon decay mechanism than by the  $q\bar{q}$  2-jet model. A deviation of these data from a 3 gluon decay mechanism may be accounted for by other  $T'$  decay modes.

Finally we have studied the angular distribution of the thrust axis of the continuum and the  $T$  and  $T'$  direct decay. This angular distribution for the  $T'$  is found to be similar to that of the  $T$ . The continuum data are consistent within 3 standard deviations with the  $q\bar{q}$  2-jet prediction. The  $T$  thrust angular distribution is in good agreement with the QCD predictions and rejects scalar gluons by more than four standard deviations.

#### ACKNOWLEDGEMENTS

We are indebted to the DORIS storage ring group and in particular to Dr. K. Wille for their efforts in support of our experiment. Our thanks are also due to the DESY-Heidelberg group which built the detector. We thank Dr. H. Lynch for useful discussions concerning the multiplicity analysis. The non-DESY members of the collaboration thank the DESY directorate for their hospitality. A.A., A.S., B.N. and T.Z. would like to thank the DESY directorate for financial support.

#### REFERENCES

- [1] Ch. Berger et al., Phys. Lett. 82B, 449 (1979)
- [2] C.W. Darden et al., Phys. Lett. 80B, 419 (1979)
- G. Alexander and H.H. Spitzer, Proceedings of the XIX. International Conference of High Energy Physics, p. 255, Tokyo (1978)
- [3] F.H. Heimlich et al., Phys. Lett. 86B, 399 (1979)
- [4] Total Width and Lepton Branching Ratio of the  $T$  (9.46), LENA Collaboration, B. Niczyporuk et al., DESY Report 80/53 (1980), Phys. Rev. Lett. 46, 92 (1981)
- [5] J.K. Bienlein et al., Phys. Lett. 78B, 360 (1978)
- C.W. Darden et al., Phys. Lett. 78B, 364 (1978)
- D. Andrews et al., Phys. Rev. Lett. 44, 1108 (1980)
- T. Böhringer et al., Phys. Rev. Lett. 44, 1111 (1980)
- [6]  $T'$  (10.01) Resonance Parameters, LENA Collaboration, B. Niczyporuk et al., DESY Report 80/81 (1980), to be published in Phys. Lett. B
- [7] W. Bartel et al., Phys. Lett. 66B, 483 (1976) and 77B, 331 (1978)
- [8] M. Kramer and H. Krasemann, Phys. Lett. 73B, 58 (1978)
- E. Eichten et al., Phys. Rev. D21, 203 (1980)
- [9] Measurement of the Decay  $T' \rightarrow T \pi^+ \pi^-$ , LENA Collaboration, B. Niczyporuk et al., DESY Report 80/125 (1980), Phys. Lett. B, to be publ.
- [10] J.E. Augustin et al., Phys. Rev. Lett. 34, 764 (1975)
- [11] R.D. Field and R.P. Feynman, Nucl. Phys. B136, 1 (1978)
- [12] K. Koller and T.F. Walsh, Phys. Lett. 72B, 227 (1977); 73B, 504 (1978) and Nucl. Phys. B140, 449 (1978)
- [13] A.H. Mueller, Phys. Rev. D4, 150 (1971)
- [14] C. Bacci et al., Phys. Lett. 86B, 234 (1979)
- [15] See for instance: K. Konishi, Rutherford Preprint RL-79-035, T241 (1979) and talk given at the XI. International Symposium on Multiparticle Dynamics, Brügge (1980)
- [16] Ch. Berger et al., Phys. Lett. 95B, 313 (1980)
- [17] K. Koller, T.F. Walsh; Phys. Lett. 72B, 227 (1977) and 73B, 504 (1978)
- [18] I.I.Y. Bigi and S. Nussinov, Phys. Lett. 82B, 281 (1979)
- [19] A. Wróblewski, Acta Phys. Pol. B4, 857 (1973)



- [20] A. Fridman, Proceedings of the VIII. International Symposium on Multiparticle Dynamics, p. A129, Kayzersberg (1977)
- [21] J. Withmore, Phys. Rep. 27C, 187 (1976)
- [22] S. Barshay et al., Phys. Rev. D15, 2702 (1977)
- Huan Lee, Phys. Rev. Lett. 30, 719 (1973); G. Veneziano, Phys. Lett. 43B, 413 (1973); Chan Hong-Mo and J.E. Paton, Phys. Lett. 46B, 228 (1973)
- [23] J. Dias de Deus, Multiparticle Production and Long Range Correlations in  $e^+e^-$  Annihilations and pp High Energy Collisions, Lisboa Preprint CFMC E-7/80(1980)
- [24] See for instance: A. Fridman, Serial of Lectures Notes on High Energy Physics, No. 11, published by the Centre de Recherches Nucléaires de Strasbourg (1976) and references quoted therein.
- [25] Z. Koba, H.B. Nielsen and P. Olesen, Nucl. Phys. B40, 317 (1972)
- [26] K. Koller, H. Krasemann and T.F. Walsh, Z. Physik C1, 71 (1979)
- [27] K. Koller and H. Krasemann, Phys. Lett. 88B, 119 (1979).

TABLE 1: The number of events and the corresponding luminosities for the different energy intervals. For the continuum the weighted average CM energy  $\langle\sqrt{s}\rangle$  is also given.

$\sqrt{s}$ (Mev)	Number of Observed Events	Luminosities (nb $^{-1}$ )
7,350 - 7,490	524	176
$\langle\sqrt{s}\rangle = 7,448.8$		
8,629 - 9,142	1152	459
$\langle\sqrt{s}\rangle = 8,861.7$		
9,150 - 9,410	1226	541
$\langle\sqrt{s}\rangle = 9,275.6$		
$T'_{\text{off}}$	916	356
$\langle\sqrt{s}\rangle = 9,514.9$		
$T'_{\text{off}}$	1075	424
$\langle\sqrt{s}\rangle = 9,990.3$		
$T'_{\text{on}}$	5223	586
9,462.4		
$T'_{\text{on}}$	2814	632
10,014.8		

TABLE 3: The average  $T'$  for the  $T$  and  $T'$  decay data and for their nearby continuum data

	$\langle T' \rangle$
$T'_{\text{off}}$	$0.777 \pm 0.004$
$T'_{\text{off}}$	$0.771 \pm 0.003$
$T'_{\text{dir}}$	$0.718 \pm 0.035$
$T'_{\text{dir}}$	$0.722 \pm 0.026$

Energy Region (GeV)	Observed Average $\langle n \rangle$	UNFOLDED MOMENTS			
		$\langle n \rangle$	D	$f_2^-$	D/ $\langle n \rangle$
$\sim 7.4$	$5.59 \pm 0.09$	$6.27 \pm 0.13$	$2.39 \pm 0.08$	$-1.71 \pm 0.13$	$0.38 \pm 0.01$
$\sim 8.9$	$6.04 \pm 0.07$	$7.08 \pm 0.11$	$2.55 \pm 0.09$	$-1.92 \pm 0.13$	$0.36 \pm 0.01$
$\sim 9.3$	$6.13 \pm 0.07$	$7.28 \pm 0.11$	$2.64 \pm 0.09$	$-1.90 \pm 0.13$	$0.36 \pm 0.01$
$T'_{\text{off}}$	$6.33 \pm 0.08$	$7.57 \pm 0.15$	$2.80 \pm 0.11$	$-1.83 \pm 0.19$	$0.37 \pm 0.02$
$T'_{\text{off}}$	$6.48 \pm 0.07$	$7.67 \pm 0.12$	$2.60 \pm 0.08$	$-1.70 \pm 0.14$	$0.34 \pm 0.01$
$T'_{\text{dir}}$	$7.21 \pm 0.32$	$8.12 \pm 0.11$	$2.90 \pm 0.08$	$-1.96 \pm 0.16$	$0.36 \pm 0.02$
$T'_{\text{dir}}$	$7.49 \pm 0.30$	$8.93 \pm 0.26$	$3.18 \pm 0.15$	$-1.94 \pm 0.67$	$0.36 \pm 0.02$

TABLE 2: The observed average charged multiplicities and the unfolded statistical moments for various CM energy regions. The errors are statistical only.

## FIGURE CAPTIONS

- Fig. 1 The average charged multiplicity as a function of the CM energy. The PLUTO data are from Ref. 16. The JADE and TASSO data are from Phys. Lett. 89B, 418 (1980) and Phys. Lett. 88B, 171 (1979). The SLAC data points are from J.L. Siegrist, Ph.D. Thesis, SLAC-225 (1980). The errors are statistical only and the  $K_S^0 \rightarrow \pi^+ \pi^-$  decays are included in the plot.
- Fig. 2 The dispersions  $D$  (Fig. 2a) and the  $f_2^-$  moment (b) as a function of the average charged multiplicity. The full line in (a) is obtained by fitting the data with the expression  $D = A\langle n \rangle + B$ . In (b) the line is obtained by extrapolating low energy ( $\langle n \rangle < 7$ )  $\bar{p}p$  annihilation data (Ref. 20).
- Fig. 3 The multiplicity data plotted in the KNO form. Here  $P_n$  is the probability to observe an  $n$  prong event.
- Fig. 4 The normalized  $\cos \delta$  distributions for  $T_{\text{off}}$  (a),  $T'_{\text{off}}$  (b),  $T$  direct (c) and  $T'$  direct (d) data. Here  $\delta$  is the opening angle between pairs of tracks. The dashed and the full lines are the predictions of the two jet  $q\bar{q}$  and 3-gluon models, respectively.
- Fig. 5 The scatter plot of  $T'$  versus the real thrust  $T_{\text{ch}}$  for 3-gluon Monte Carlo events generated at 9.4 GeV.
- Fig. 6 The  $T'$  distribution for the  $T_{\text{off}}$  (a),  $T'_{\text{off}}$  (b) and the  $T$  (c) and the  $T'$  direct decay (d) data. The dashed and full lines represent the predictions obtained from the 2-jet  $q\bar{q}$  and the 3-gluon decay models, respectively.
- Fig. 7 The thrust angular distribution for (a) the combined continuum data between 9 and 10 GeV, (b) the  $T$  direct and (c) the  $T'$  direct data. The full line is obtained by fitting the data with an  $1 + \alpha \cos^2 \theta$  expression. The dashed and dashed-dotted lines are the predictions obtained for vector and scalar gluons, respectively.

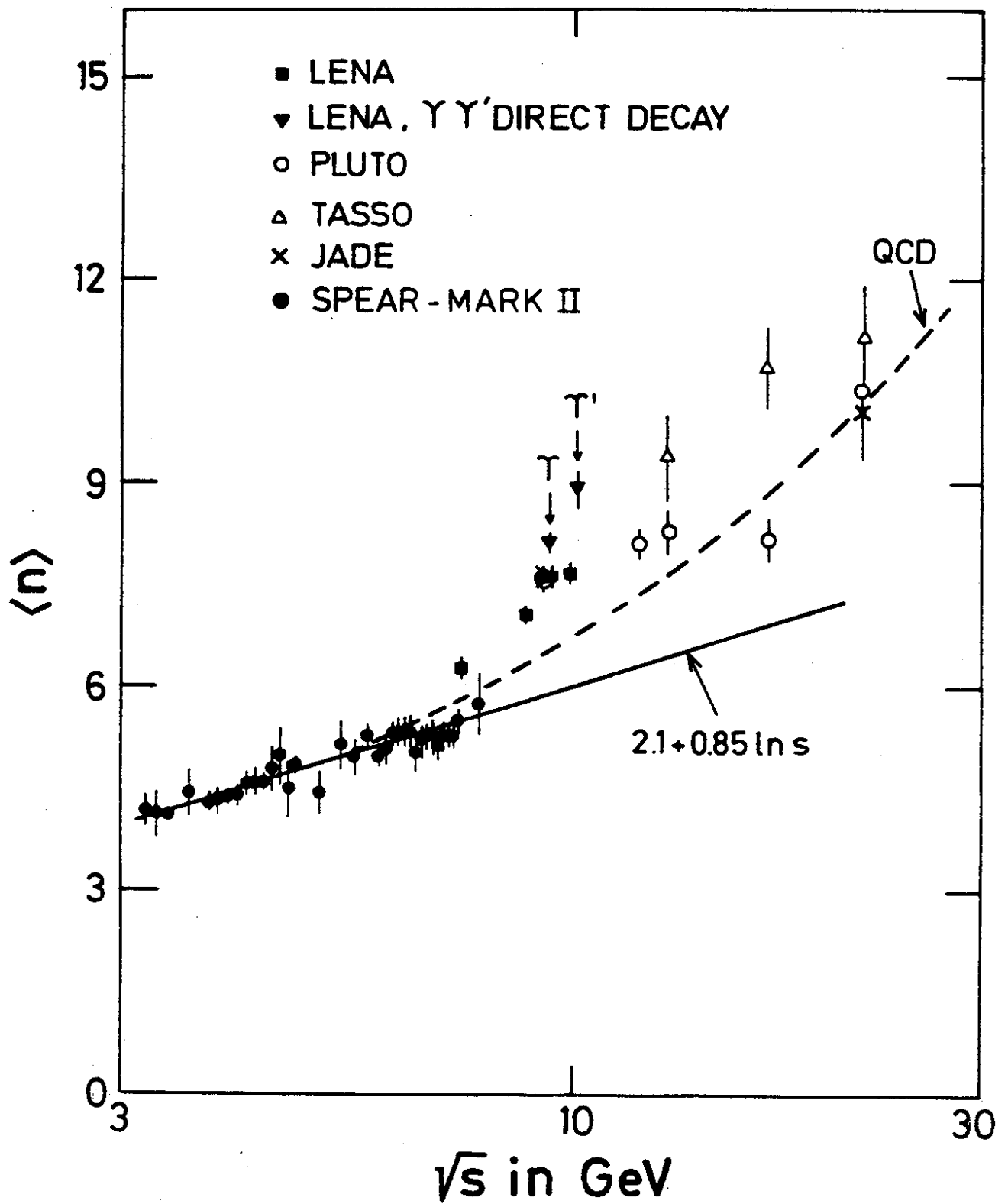


FIG. 1

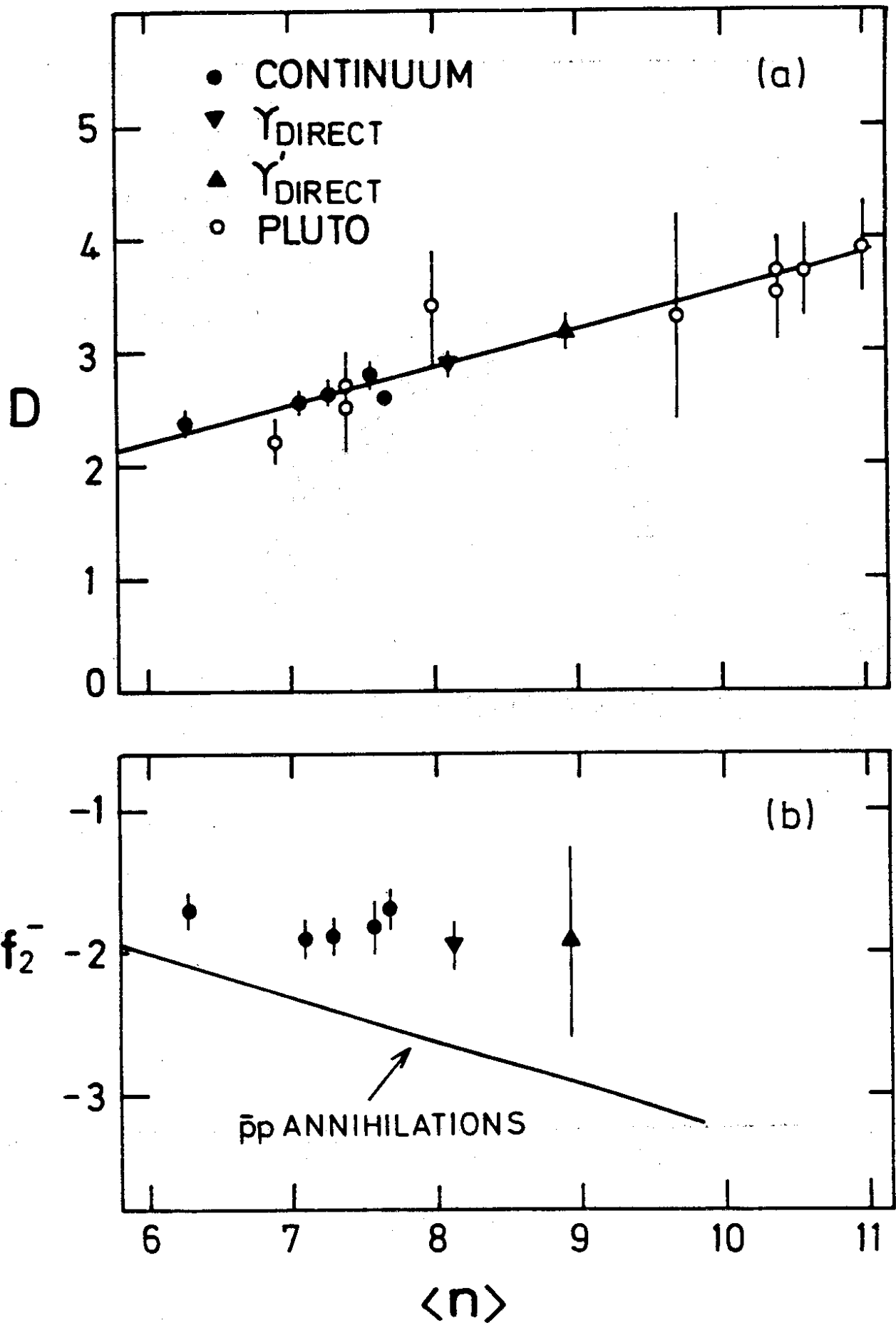


FIG. 2

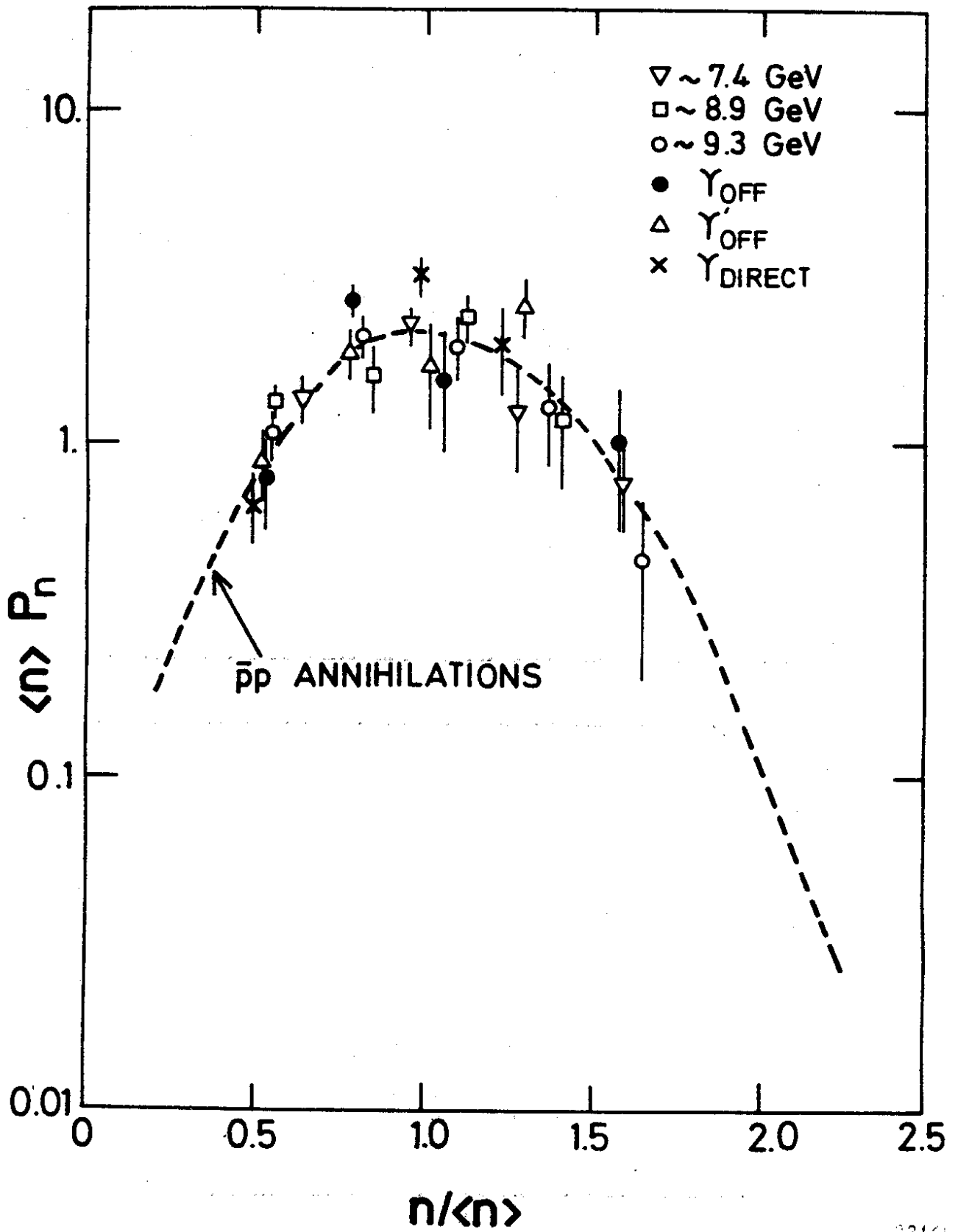


FIG. 3

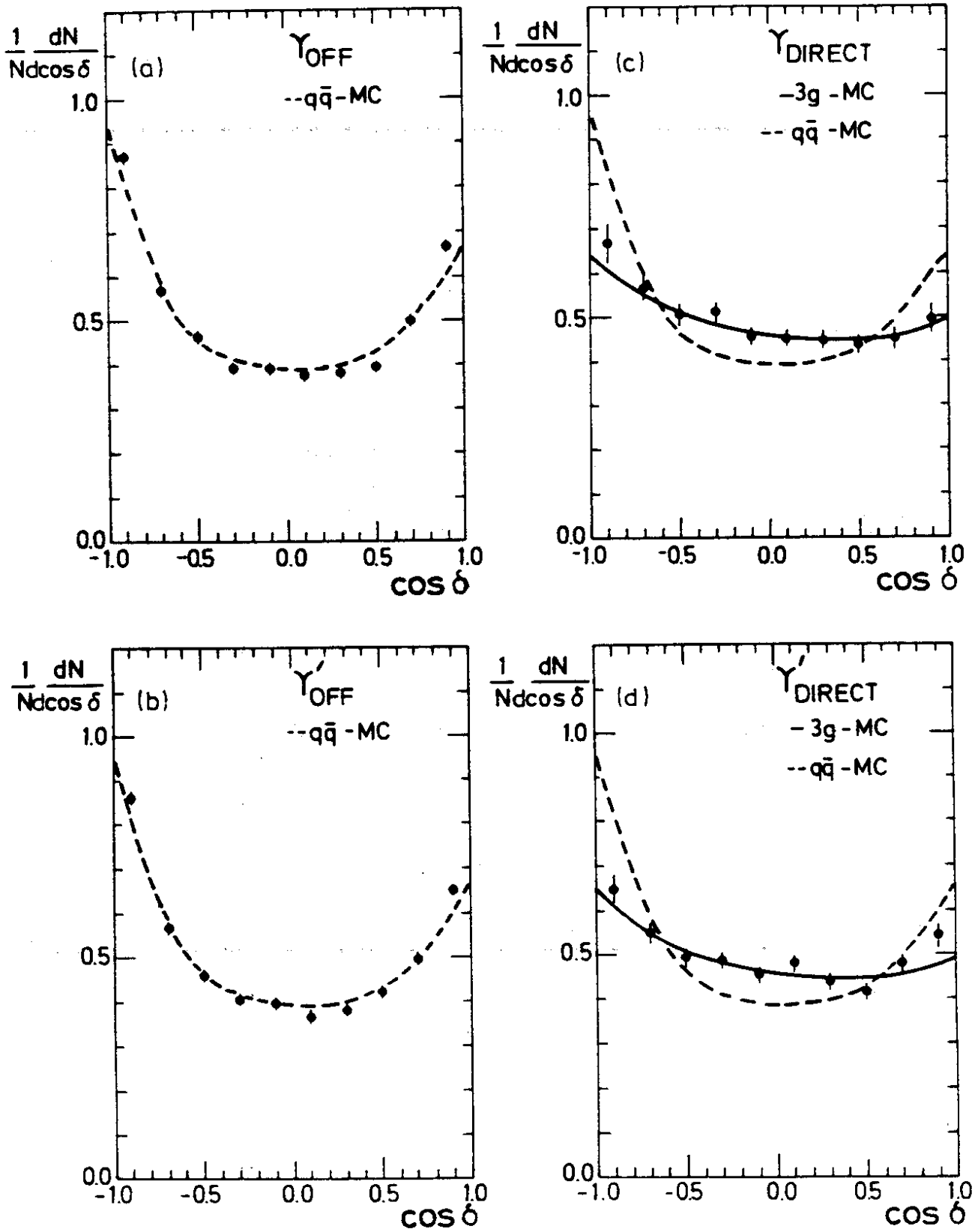


FIG. 4

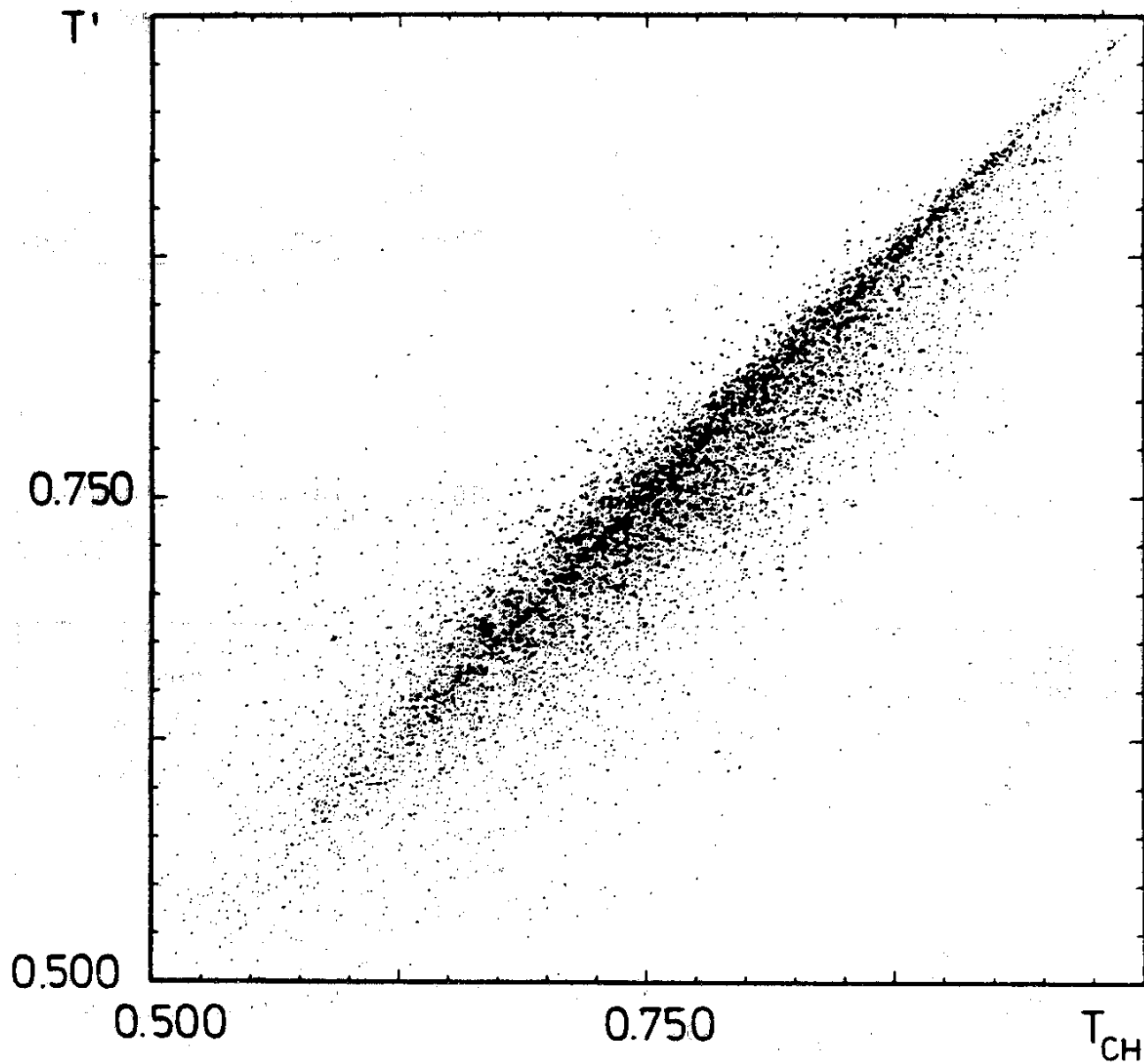


FIG. 5



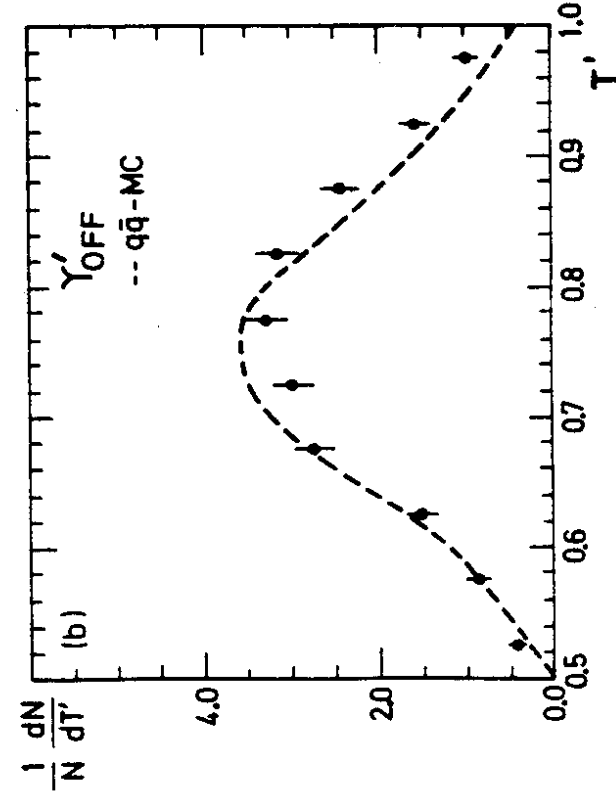
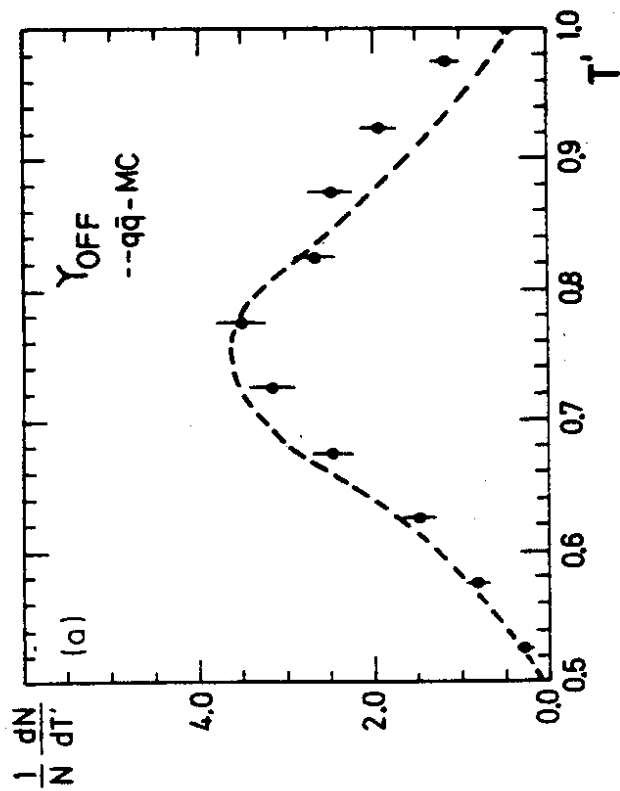
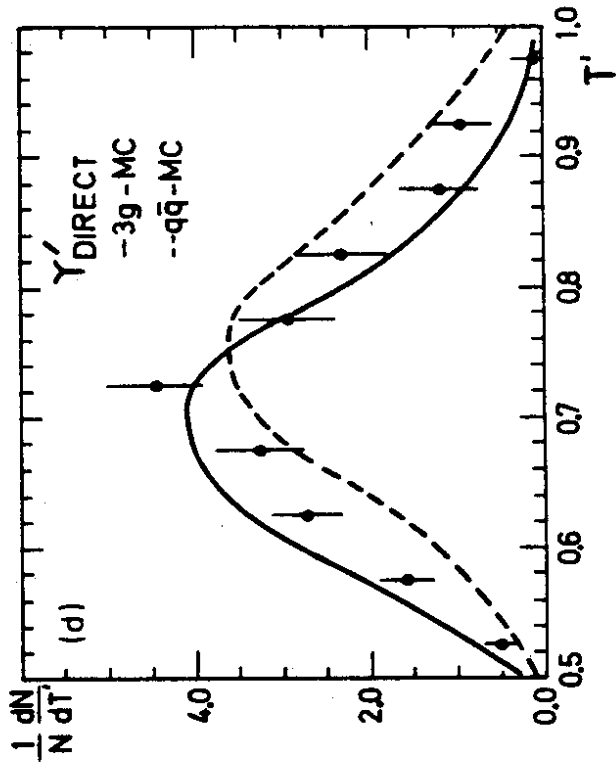
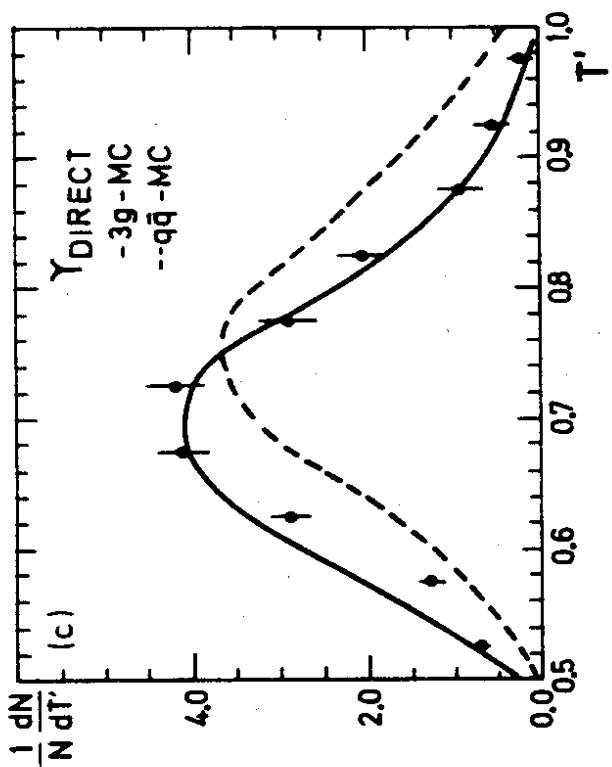


FIG. 6

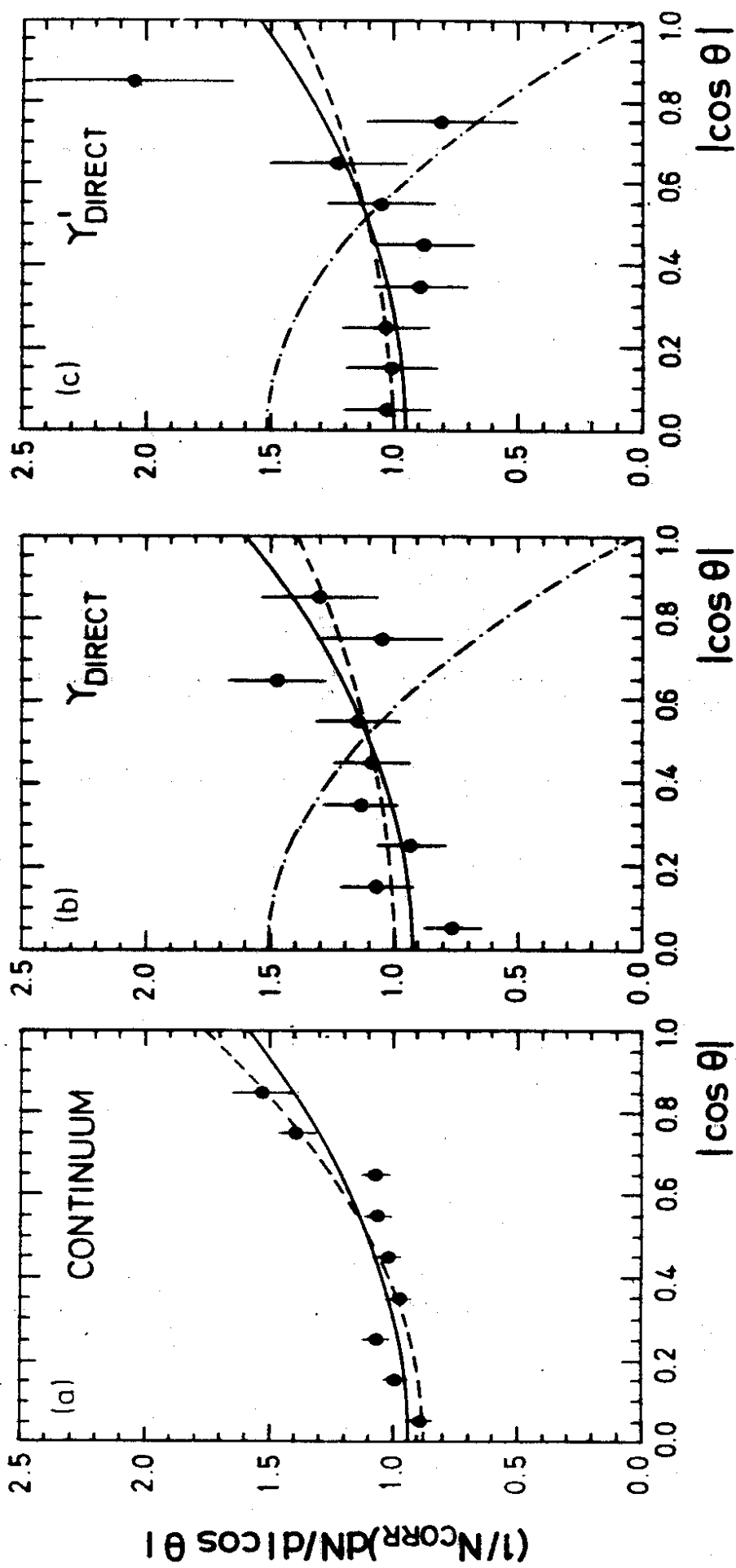


FIG. 7